Proposal of short armature core double-sided transverse flux type linear synchronous motor

Shin Jung-Seob [*1], Takafumi Koseki [*1] and Kim Houng-Joong [*2]

Linear motors have been a great interest from industries. Especially, linear synchronous motor that uses rare earth permanent magnets in the field side (PMLSM) has contributed to the popularization in industrial fields because of its high efficiency and compact size. However, the thrust force density could not be largely enhanced in conventional PMLSM due to the space competitions between the stator teeth and armature conductors. In recent years, the transverse flux PM-type linear synchronous motor has been researched as alternative because it can inherently offer high thrust density. The authors propose a short armature core double-sided transverse flux type PMLSM. In this paper, the concept and structure of the proposed model are introduced and its characteristics are both theoretically analyzed and numerically computed by field calculation using Finite Element Method (FEM).

Keywords: Linear synchronous motor, high thrust density, transverse flux type machinery, double-sided type.

1. Introduction

Linear motors are being employed increasingly in industrial fields. Such direct devices offer many advantages over ball-skrew drive, which result in a higher dynamic performance and reliability.

There are many types of linear motors including linear synchronous motor, linear induction motor and linear stepping motor etc. Especially, linear synchronous motor that uses permanent magnets (PMLSM) in the field side has contributed to the popularization in industrial fields because of the advent of rare earth permanent magnet [1]. In general, characteristics required to PMLSM in industrial fields are high thrust, high positioning accuracy and simple structure etc.

Especially, how to obtain high thrust density is one of the most significant investigation subject today. The transverse flux type machinery is an ideal alternative.

It has some advantages distinguished from other types of motors. Most importantly, there is no competition between the space requirement of flux carrying core irons and the space occupied by armature windings.

This increases the design flexibility compared with the longitudinal flux type machinery, in which there is a fundamental competition between the stator teeth and armature conductors. The other advantage of the transverse flux type machinery is that it can increase the thrust density with increase in the pole number or decrease in the pole pitch in designated dimension.

However, conventional transverse flux type machinery has such complex manufacturing requirements that it is impractical for industrial production [2].

For that reason, the authors propose short armature core double-sided transverse flux type PMLSM. In this paper, the concept and structure of the proposed model are introduced and its characteristics are both theoretically analysed by magnetic circuit method and numerically computed by field calculation using FEM.

Correspondence: Department of Electrical Engineering, The university of tokyo, 7-3-1, Hongo, Bunkyo-Ku, Tokyo 113-8656, Japan

email: jungseobshin1008@koseki.t.u-tokyo.ac.jp

[*1] The University of Tokyo [*2] Sung-Jin Royal Motion Co. Ltd

2. Short armature core double-sided transverse flux type PMLSM

2.1 Point of new motor design

There are many technical performance required to PMLSM in the industrial fields, including high thrust, low detent force, low cost etc. In development stage, the following was significant point for the authors.

(1) High thrust density
(2) Low detent force
(3) Structurally compensated normal attractive force
(4) Simple structure, easy design and production

2.2 Basic structure and the operational principle of the proposed model

Fig. 1 shows fundamental configuration of three-phase unit of the proposed model.

An armature unit consists of two armature core that has square shape, four armature coil in order to generate travelling field and non-magnetic material box.

The square-shaped armature core has basically two salient poles and can be simply fabricated by laminated steel, which is a large improvement compared with conventional transverse flux machine that has complex structure. Also, it is simply inserted to non-magnetic material box, which results in simple assembly.

Four armature coils are wound around each salient pole as shown in Fig. 1 (a). Since it is enough to insert armature coils to each salient pole, armature core is not needed to be segmented in order to save space for winding. For that reason, simplification of components and easy production will be achieved.

In the field side, an field unit consists of four magnets, two back yokes as shown in Fig. 1 (b). The back yoke can be also simply fabricated by laminated steel, which results in simple structure and manufacturing.

An magnetic circuit has achieved in the proposed model as shown in Fig. 1 (c) by inserting an armature unit to an field unit. The flux leakage can be reduced by placing field magnets on the surface of back yoke and a short air gap length. Also, the magnetic flux linking an armature coil is not reduced largely because the armature coils is closed to the field magnet. This short flux path can make motor more compactly and increase the back electromotive force, which results in an increase of a thrust density.

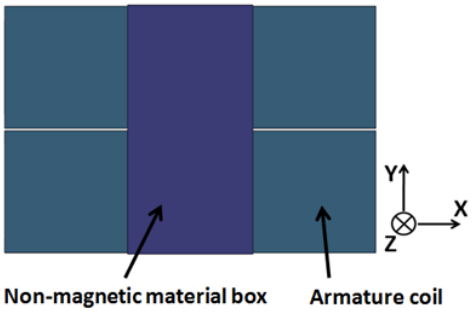

(a) An armature unit

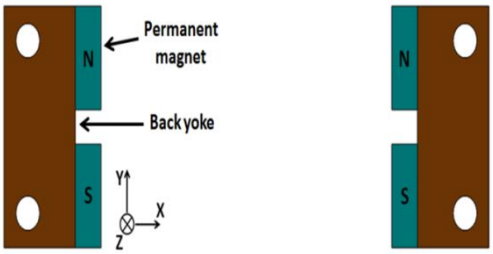

(b) An field unit

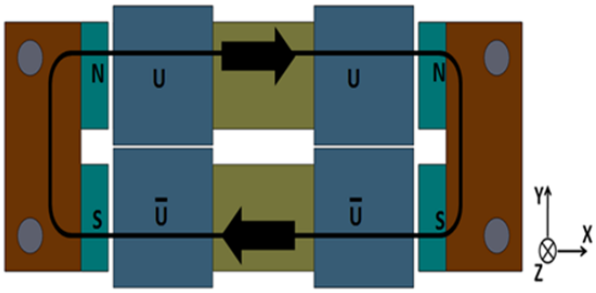

(c) An magnetic circuit

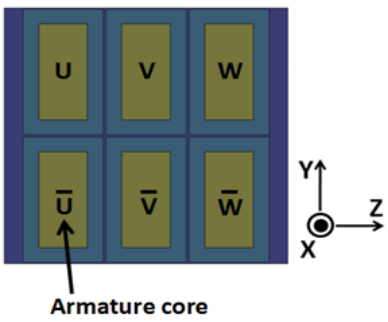

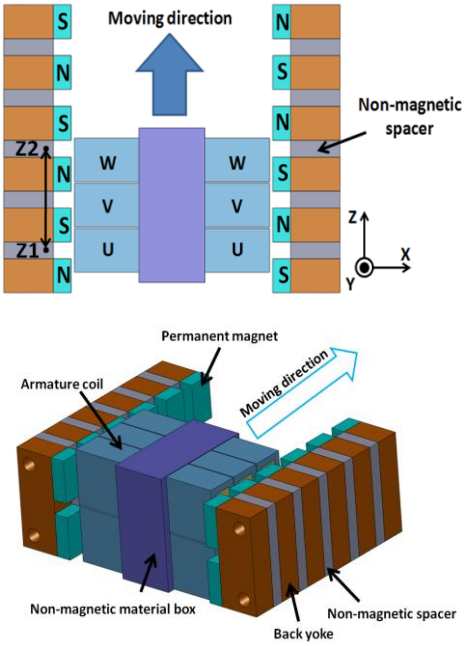

(d) Configuration to the moving direction

Fig. 1. Fundamental configuration of three-phase units (Significant points in Fig. 1(d) are marked on the graphs in Fig. 8 and Fig. 9.).

Also, strong normal attractive force between the armature side and the field side can be cancelled in principle because of double-sided type structure.

In moving direction, armature cores are arranged to moving direction Z as shown in Fig. 1 (d). Each armature core is apart with 120 degrees spatially.

The back yoke is arranged to the moving direction Z with non-magnetic spacer and each magnet is apart with 180 degrees electrically. This non-magnetic material spacer between cores in the armature and field side can achieve magnetic separation of each core.

By adding AC current which has 120 degree phase difference to each armature core, the proposed motor drives as three-phase AC synchronous machinery. The distance between point Z1 and point Z2 in Fig. 1(d) is a mechanical period in the moving direction.

Fig. 2 shows three-floor configuration of the proposed model.

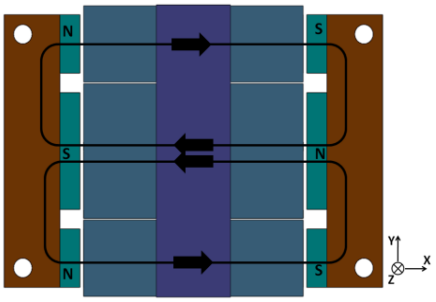

Fig. 2. Three-floor configuration.

Depending on purpose and required size, it is possible to fabricate three-floor configuration. In this manner, not only three-floor but four, five and six floor configuration are achieved in the proposed model. By increasing a number of floors, an increase of a thrust could be achieved because of an increasing area in which thrust is generated.

3. Theoretical evaluation of the fundamental characteristics in the proposed model

The authors have employed magnetic circuit method in order to conduct simple design and estimate fundamental characteristics theoretically [3].

In the proposed model, a armature core consists of a magnetic circuit as shown in Fig. 1(c) when an armature side is in a field side. In order to estimate characteristics of the proposed model simply, the authors have considered one magnetic circuit as shown in Fig. 3. Also, they assumed the permeability of armature and field cores are infinitely large.

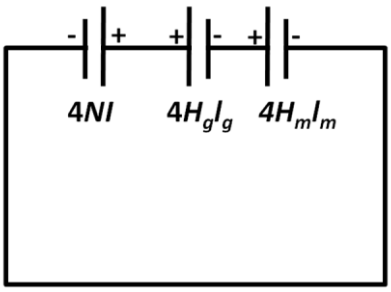

Fig. 3. Equivalent magnetic circuit considering an magnetic circuit.

3.1 The air gap flux density

From Fig. 3, an magnetic circuit can be expressed as

$$NI = H_g l_g + H_m l_m \quad [\mathrm{A}] \tag{1}$$

where H_m, H_g are the magnetic-field component of magnet and the air gap, l_g, l_m is the length of the air gap and magnet, I is armature current and N is the turn number of a winding of an armature pole.

If the permeability of armature and field cores is infinite, the magnet flux density B_m in operating point can be expressed as (2). B_r is remanence of magnet and μ_0 is permeability of the air gap.

$$B_m = B_r + \mu_0 H_m \quad [\mathrm{T}] \tag{2}$$

Also, the air gap flux density B_g, the air gap flux ϕ_g and the magnet flux ϕ_m can be calculated (3)-(5). In (4) and (5), A_m, A_g are the dimension of magnet and air gap.

$$B_g = \mu_0 H_g \quad [\mathrm{T}] \tag{3}$$

$$\phi_g = B_g \times A_g \quad [\mathrm{Wb}] \tag{4}$$

$$\phi_m = B_m \times A_m \quad [\mathrm{Wb}] \tag{5}$$

By using (1) - (5), The air gap flux density B_g can be written as (6).

$$B_g = \frac{B_r}{\frac{A_g}{A_m}+\frac{\mu_0 g_c}{l_m}}\left(1 - \frac{NI}{H_c l_m}\right) \quad [\mathrm{T}] \tag{6}$$

In (6), H_c is the coercive force of magnet, g_d is the air gap length considered cater coefficient.

3.3 The back Electromotive Force (EMF)

If the air gap flux distribution can be modeled as shown in Fig. 4 by moving an armature unit, the air gap flux and its density can be expressed by fourier series. Its fundamental component is expressed as (7).

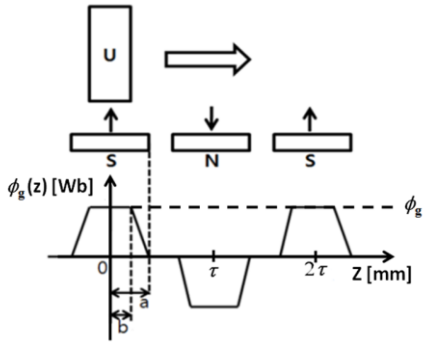

Fig. 4. The air gap flux distribution by moving an armature unit.

$$\phi_g(z) = \frac{4k_l\phi_g\tau}{(b-a)\pi^2}\left\{\cos\left(\frac{\pi a}{\tau}\right) - \cos\left(\frac{\pi b}{\tau}\right)\right\}\cos\left(\frac{\pi z}{\tau}\right)$$

$$= k_l\phi_{gmax}\cos\left(\frac{\pi z}{\tau}\right) \quad [\mathrm{Wb}]$$

$$B_g(z) = \phi_g(z)A_g = k_l B_{gmax}\cos\left(\frac{\pi z}{\tau}\right) \quad [\mathrm{T}] \tag{7}$$

In (7), $\emptyset_{gmax}$, B_{gmax} are the maximum value of the air gap flux and its density, k_l is flux leakage coefficient, τ is pole pitch, a and b are the half length of one field magnet and one armature core respectively.

Hence, the back EMF and its root mean square (RMS) value can be obtained as (8). In (8), p is the number of magnetic circuits in an unit, v is the moving velocity and z is the distance to moving direction.

$$e\,(z) = -k_c pN\frac{d\phi_g}{dt} = \frac{k_c k_l \pi v p N \phi_{gmax}}{\tau}\sin\left(\frac{\pi z}{\tau}\right)[\mathrm{V}]$$

$$E_{rms} = \frac{0.707 k_c k_l \pi v p N \phi_{gmax}}{\tau} \quad [\mathrm{V}] \tag{8}$$

3.3 Detent force

With regard to calculation of detent force, the authors employed virtual work principle. Detent force of an armature unit can be expressed as (9).

$$F_{detent}(z) = -\frac{dW}{dz} = -\frac{d}{dz}\left(\frac{B_g^2(z)V_g}{2\mu_0}\right)$$

$$= \frac{k_l^2 B_{gmax}^2 \pi A_g g_d}{2\mu_0 \tau}\sin\left(\frac{2\pi z}{\tau}\right) = F_d \sin\left(\frac{2\pi z}{\tau}\right) \quad (9)$$

In (9), V_g is the air gap volume. It is found that the period of detent force is the same with pole pitch τ electrically.

The reduction of detent force in PMLSM is one of the most important factors required in industrial fields and this can affect to high positioning accuracy. Many methods to reduce detent force in PMLSM have been reported included in skewing, semi-closed slots and magnet length optimization etc. However, these methods can be a burden in the manufacturing stage and sometimes affect to manufacturing cost.

The authors focused on slot-pole combination to reduce detent force because the authors had focused on simple structure, easy design and production. In the case of rotational synchronous machinery, the higher Least Common Multiple (LCM) of slot-pole is, the lower cogging torque can be achieved.

Since drive principle of linear synchronous machine is the same with that of rotational synchronous machine, the authors applied nine slot-eight pole combination to the proposed model in the stage of selecting numbers of armature cores and field poles [4]. Hence, nine armature cores are faced with eight magnets in a electric period.

3.4 Static Longitudinal Force

Static longitudinal force of an armature unit in the proposed model is (10).

$$F_{static}(z) = \frac{k_l^2 B_{gmax}^2 \pi A_g g_d}{2\mu_0 \tau}\sin\left(\frac{2\pi z}{\tau}\right) + \frac{0.707 p \pi k_c k_l N I \phi_{gmax}}{\tau}\sin\left(\frac{\pi z}{\tau}\right)$$

$$= F_d \sin\left(\frac{2\pi z}{\tau}\right) + F_t \sin\left(\frac{\pi z}{\tau}\right) \quad [\mathrm{N}] \qquad (10)$$

The first term is detent force expressed in (9) and the second one is thrust of the proposed model. It is found that only detent force exists when *I* is 0.

Thrust is proportional to the air gap flux ϕ_{gmax}, applied magnetomotive force *NI* and inversely proportional to the pole pitch τ in the proposed model. In contrast with longitudinal flux machinery, increasing pole pairs in designated dimension results in a decreased pole pitch. This decreased pole pitch does not reduce the magnetic flux linking armature coil, which increases the back EMF with the rapid change of the flux for the same mover speed and results in drive as transverse flux type linear motor [5]. Hence, a higher thrust density can be achieved by optimizing pole pitch in the proposed model.

The thrust considered nine slot-eight pole combination can be expressed as (11). In (11), θ is the number of each armature core in nine slot-eight pole combination. The main parameters for theoretical calculation and results of fundamental characteristics are shown in Table 1.

$$F_{thrust}(z) = \sum F_t \sin\left(\frac{\pi z}{\tau} + 2(\theta - 1)\right), (\theta: 1\sim 9)[N] \quad (11)$$

Table 1 The main parameters for theoretical calculation and results of fundamental characteristics.

An armature core size [mm]	59.2w×15h×7d
An field core size [mm]	15w×35h×9d
An magnet size [mm]	5.4w×15h×9d
The dimension of the air gap in an magnetic circuit A_g [mm^2]	135
The dimension of magnet in an magnetic circuit A_m [mm^2]	135
The flux leakage coefficient k_l	1
Pole pitch τ [mm]	13.5
The winding factor k_c	0.88
The number of magnetic circuits in an unit *p*	1
Moving velocity *v* [m/s]	1
Magnetomotive force per an salient pole *NI* [AT]	335
The air gap flux density at no load B_g [T]	1.088
The air gap flux at no load ϕ_g [Wb]	2.136×10^{-4}
The RMS value of back EMF E_{rms} [V]	8.28
The maximum detent force in an armature unit F_d [N]	36.21
The maximum thrust in an armature unit F_t [N]	41.44
The maximum thrust in 9core-8pole combination F_{thrust_max} [N]	178.98

4. Numerical performance evaluation of the proposed model using FEM

The authors applied three-dimensional FEM analysis to the proposed model for rational verification of fundamental characteristics. Table 2 shows the materials used in FEM analysis and Fig. 5 represents the *B-H* curves of 50JN230 [6]-[7].

Table 2 Specification of the material used in FEM analysis.

Armature core	50JN230 (JFE-steel Corp.)
Field core	50JN230 (JFE-steel Corp.)
Permanent magnet	N50M (Shinetsu Chemical.) (NdFeB,H_c:1092436A/m,B_r:1.32T)
The current density of armature coil [A/mm^2]	7
The diameter of armature coil [mm]	0.804×0.804(conductor:0.7×0.7)

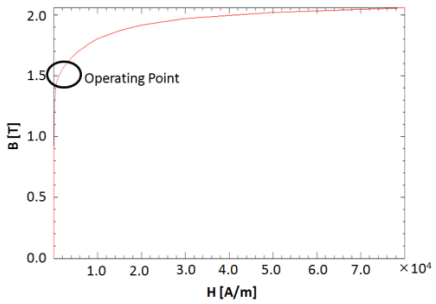

Fig. 5. B-H curve of 50JN230 (JFE Steel Corp.)

4.1 The air gap flux density

Fig. 6 shows one of the results of the flux density distribution in the proposed model at no load. In three-dimensional FEM analysis considered saturation of core, the maximum flux density in the air gap was 1.068T. Also, the flux density is distributed in the overall region. It means that the occupancy ratio of iron core is high in the proposed model, which results in an increase of thrust density because of low wasted space.

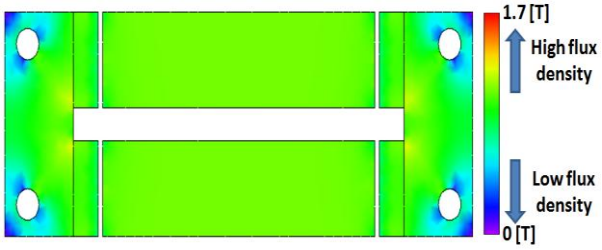

Fig. 6. Flux density distribution of the proposed model.

Fig. 7 shows the comparison of the air gap flux density by moving an armature unit. The maximum air gap flux density in theoretical calculation was nearly the same with three-dimensional FEM value. Also, its wave form was nearly sinusoidal. From this result, the authors has decided the flux leakage coefficient k_l as 0.98.

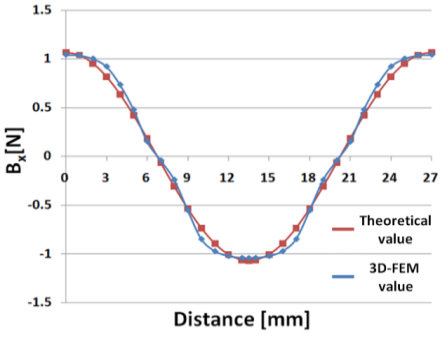

Fig. 7. The air gap flux density.

4.2 Detent force

The result of detent force in three-dimensional FEM analysis is shown in Fig. 8.

The maximum detent force considered three armature cores per one phase was 88.7N, which is nearly the same with the theoretical value considered the flux leakage coefficient k_l.

The maximum value of total detent force considered nine slot-eight pole combination could be reduced to about 2.3N.

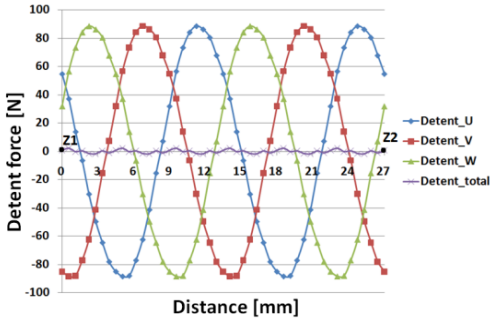

Fig. 8. Detent force.

4.3 Static Longitudinal Force

Fig. 9 shows the result of static longitudinal force considered three armature cores per a phase at 335AT.

As shown in Fig. 9, the maximum value of static longitudinal force and thrust was 167.58N and 114.76N respectively. When considering nine slot-eight pole combination, the maximum value of thrust is 172.14N, which is nearly the same with the theoretical value considered the flux leakage coefficient k_l. In this point, detent force was 1.35% of total thrust, which means a high positioning accuracy could be achieved in the core-typed proposed model.

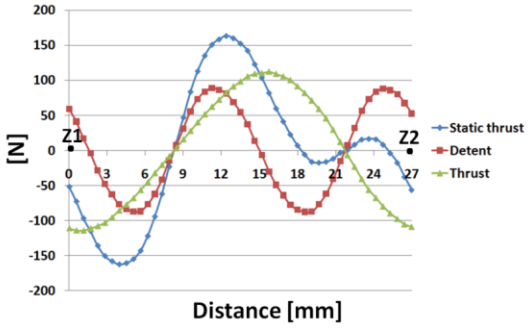

Fig. 9. Static thrust, detent force and thrust.

Fig. 10 shows thrust per three-phase with the variation of magnetomotive force. As the armature current increases, the incremental ratio of the thrust decreases due to the saturation effect of core irons.

Also, thrust was 120.17N in rated region in which magnetomotive force is 244.8AT.

However, it is found that the rated region is relatively lower compared with saturation region. From the result of static longitudinal force considered three armature cores per one phase as shown in Fig. 11, it is found that high static longitudinal force is highly affected by not electric load but magnetic load. An optim-

al design considered a balance between the electric and magnetic loading is needed in order to decrease low detent force per an phase and improve rated thrust.

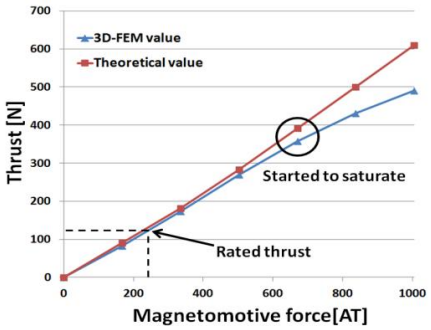

Fig. 10. Thrust-current characteristics.

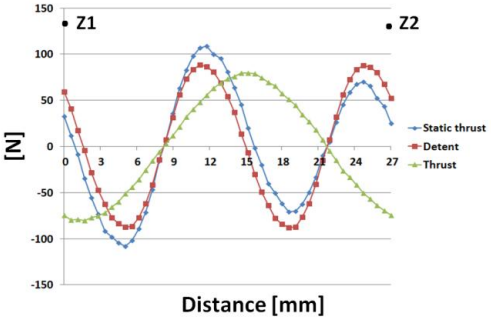

Fig. 11. Static thrust, detent force and thrust in rated region.

4.5 Thrust density

The authors calculated thrust density based on the following. Rated thrust is used in calculation. Table 3 shows the thrust density in the proposed model.

(1) The total volume in which the armature side is faced with the field side.
(2) The total dimension in which thrust is generated.
(3) The total weight of magnet used in area in which thrust is generated.
(4) The total weight of mover included in coil mass, non-magnetic material.

Table 3 The results of thrust density.

The total volume [m^3]	0.43×10^{-3}
The thrust density based on volume [N/m^3]	279.47×10^{3}
The total dimension [m^2]	8.64×10^{-3}
The thrust density based on dimension [N/m^2]	13.91×10^{3}
The total weight of magnet [kg]	0.18
The thrust density based on weight of magnet [N/kg]	667.6
The total weight of mover [kg]	1.82
The thrust density based on weight of mover [N/kg]	65.9

5. Conclusion

In this paper, short armature core double-sided transverse flux type PMLSM is proposed.

Also, its characteristics are theoretically calculated by magnetic circuit method and numerically analyzed by FEM. Especially, the details of the theoretical calculation allowed for simple design and understanding of the fundamental characteristics of the proposed model without complex calculation.

In this research, it is found that the proposed short armature core double-sided transverse flux type PMLSM has the following advantage.

(1) High thrust density can be achieved by transverse flux type structure, low flux leakage, short flux path and high occupancy ratio of space.
(2) A high positioning accuracy could be achieved in the core-typed proposed model by reducing detent force to 1.35% of thrust with nine slot-eight pole combination.
(3) Strong normal attractive force between the armature side and the field side can be cancelled by applying double-sided type structure.
(4) Simple structure, easy design and production can be achieved by employing the lamination of square-shaped iron core, non-magnetic material and easy winding work, which is a large structural improvement compared with conventional transverse flux machine.

Future work will involve an optimal design in order to balance the electric and magnetic loading. Also, further characterization of the prototype model through static and dynamic testing including thrust, thrust ripple and positioning accuracy shall be done.

References

[1] Shin Jung-Seob, Takafumi Koseki, Kim Houng-Joong : "The design of flux concentrated type transverse flux cylindrical PMLSM for high thrust", The International Symposium on Linear Drives for Industry Applications (LDIA2011),Netherlands, 2011.
[2] Zou. J. B, Wang. Q : "Fundamental Study on a Novel Transverse Flux Permanent Magnet Linear Machine", Proceedings of the International Conference on Electrical Machines, pp. 2894-2898, 2008.
[3] Krishnan Ramu : "Permanent Magnet Synchronous and Brushless DC Motors", CRC Press/Taylor & Francis, 2009.
[4] T. Kenjo, S. Nagamori : "Brushless motors : advanced theory and modern applications", Sogo Electronics Press, 2003.
[5] Weh. H, Hoffman. H, Landrath. J : "New Permanent Magnet Excited Synchronous Machine with High Efficiency at Low Speeds", Proceedings of the International Conference on Electrical Machines, 1988.
[6] JFE Steel Corp. http://www.jfe-steel.co.jp/
[7] Shinetsu Chemical Co. Ltd. http://www.shinetsu.co.jp/j/